METHANE AS A DIAGNOSTIC TRACER OF CHANGES IN THE BREWER-DOBSON
CIRCULATION OF THE STRATOSPHERE

Ellis E. Remsberg

Science Directorate

NASA Langley Research Center

21 Langley Blvd., Mail Stop 401B

Hampton, VA 23681, USA

Ellis.E.Remsberg@nasa.gov

Abstract. This study makes use of time series of methane (CH_4) data from the Halogen Occultation Experiment (HALOE) to detect whether there are any statistically significant changes of the Brewer-Dobson Circulation (BDC) within the stratosphere during 1992-2005. The HALOE CH_4 profiles are in terms of mixing ratio versus pressure-altitude and are binned into latitude zones within the southern and the northern hemisphere, and their separate time series are then analyzed using multiple linear regression (MLR) techniques. The CH_4 trend terms for the northern hemisphere are positive at 10°N from 50 hPa to 7 hPa and significantly larger from 20 hPa to 7 hPa than the tropospheric CH_4 trends of about 3%/decade. At 60°N the trends are clearly negative from 20 hPa to 7 hPa. Their combined trends indicate an acceleration of the BDC for the northern hemisphere during those years, most likely due to changes from the effects of wave activity. No similar significant acceleration is found for the southern hemisphere. Trends from HALOE H_2O are analyzed for consistency. Their mutual trends with CH_4 are anti-correlated qualitatively in the middle and upper stratosphere, where CH_4 is chemically oxidized to H_2O. Conversely, their mutual trends in the lower stratosphere are dominated by their trends upon entry to the tropical stratosphere. Time series residuals for CH_4 in the lower mesosphere also exhibit structures that are anti-correlated in some instances with those of the tracer-like species HCl. Their occasional aperiodic structures indicate the effects of transport following episodic, wintertime wave activity. It is concluded that observed multi-year, zonal distributions of CH_4 can be used to diagnose major instances of wave-induced transport in the middle atmosphere and to detect changes in the stratospheric BDC.

1

1 Background

There is a primary, seasonal circulation in the meridional plane of the stratosphere that dynamically balances the differential heating between Equator and Pole. It is a measure of the diabatic circulation and is often termed the residual mean mass circulation or the Transformed Eulerian Mean (TEM) circulation (e.g., Dunkerton, 1978; Andrews et al., 1987). To a large degree, that primary circulation is balanced at the middle latitudes by two-way exchanges or mixing processes (Birner and Bönisch, 2011; Garny et al., 2014; Ploeger et al., 2014). Together, both mechanisms constitute the total or Brewer-Dobson circulation (BDC), generally having an upward component at low latitudes and a return, downward component at the extratropical latitudes of both the northern and the southern hemispheres (e.g., Butchart, 2014; Plumb, 2007; Haynes et al., 1991). The dissipation of planetary (or Rossby) waves and gravity wave forcings tends to accelerate the BDC and to enhance mixing in the winter hemisphere (e.g., Solomon et al., 1986; Plumb, 2007; Shepherd, 2007; Okamoto et al., 2011). Thus, it is likely that there is some asymmetry for the BDC in the northern versus the southern hemisphere stratosphere because winter wave forcing and mixing processes are more pronounced and frequent in the northern hemisphere (Shepherd, 2007).

A schematic of the BDC and its relation to the distribution of ozone in the stratosphere is shown in Fig. 1 for March, where the solid black curves represent the sense of the circulation and the vertical orange arrow represents the approximate region for the propagation of waves from the upper troposphere and up into the middle atmosphere (see Shaw and Shepherd, 2008). Figure 1 indicates that the BDC leads to an accumulation of ozone in the extratropics of the northern hemisphere by March. Tracer-like molecules, such N_2O and CH_4, exhibit distributions that are well correlated and vary seasonally in response to changes in the BDC (Plumb and Ko, 1992; Holton, 1986).

1   Figure 2 is an example of the zonally-averaged distribution of CH_4 for January from a

2   NASA/Goddard, two-dimensional chemistry and transport model simulation (Fleming et al.,

3   1999). The white arrows show the stratospheric BDC, which is strong in the winter hemisphere

4   (longer arrows) and weak in the summer stratosphere. Tracer fields such as CH_4 depict the

5   circulation, i.e., bulging upward in the tropics and downward at high latitudes (more so in the

6   winter hemisphere). Figure 2 shows that the January zonal-mean circulation is in the correct

7   sense to bring about the accumulation of ozone in the lower stratosphere by March, as shown in

8   Fig. 1. In addition, Manney et al. (1994) emphasize that the character of the observed winter

9   hemisphere transport and descent differs for the upper versus the lower stratosphere and depends

10   on whether the polar vortex is undisturbed and centered on the Pole or disturbed by Rossby-wave

11   activity.

12

13   A current issue is whether the observed, seasonal BDC is changing in the presence of the steady

14   increases in the so-called "greenhouse gases", like CO_2 (e.g., Butchart, 2014). Early on, Rind et

15   al. (1990) conducted a series of simulation studies of those effects, and their results indicated that

16   there will be an acceleration of the BDC, particularly in the northern hemisphere. Lin and Fu

17   (2013) analyzed more recent results from a collection of chemistry/climate models (CCM), and

18   they found that the diabatic effects from changes in the ozone and CO_2 are likely driving

19   observed changes in the meridional temperature gradients and of the BDC of the lower

20   stratosphere. Based on the results of the CCM studies, they decomposed the BDC into a

21   transition (100-70 hPa) branch, a shallow (70-30 hPa) branch, and a deep (30 hPa and higher)

22   branch. Further, the CCM studies predict an acceleration of the BDC that will affect the rate of

23   recovery for the ozone layer in the lower stratosphere.

24

25   Observational evidence for the diagnosis of a long-term acceleration of the several branches of

26   the BDC is not clear from time series of stratospheric temperatures (Butchart, 2014). Garcia et

27   al. (2011) recommend using observed chemical tracers that are well sampled, have linear (CO_2)

28   or exponential (SF_6) growth rates, and no chemical loss in the stratosphere. To that end, Ray et

1   al. (2014) and Ploeger et al. (2014) have successfully employed measured profiles of CO_2 and

2   SF_6 to diagnose trends in the BDC and to separate the effects of the residual circulation from the

3   effects of mixing processes. Their observations apply to pressure altitudes or potential

4   temperatures of the lower stratosphere (16 to 30 km). What about other chemical tracers? For

5   example, hydrogen fluoride (HF) is a stratospheric end product of the photochemical conversion

6   from chlorofluorocarbon (CFC) molecules but has been increasing non-linearly, so it is not a

7   good candidate for such studies. H_2O has shown long-term increases of about 0.6%/yr (Scherer

8   et al., 2008), but H_2O entering the stratosphere from below is subject to seasonal and occasional

9   episodic changes of the temperature at the tropical tropopause. CH_4 exhibits a small, monotonic,

10   and nearly linear, annually-averaged trend in the troposphere, and it is unaffected during its

11   upward transport through the tropical tropopause.

12

13   Generally, it is not possible to diagnose an acceleration of the BDC solely from a time series of a

14   chemical tracer like CH_4 because its mixing ratio, $\chi(r,t)$, at a specific location r in the

15   stratosphere is the integral of the product in expression (1) below for all past times t' from $-\infty$ to

16   t, where $\chi_0(t')$ is the time series for CH_4 in the troposphere, $G(r,t')$ is the stratospheric age spectra

17   or transit time distribution (its first momentum being the age of air), and $L(r,t')$ is its loss

18   function that depends on the path spectra and the chemical sink distribution for CH_4 in the

19   stratosphere (Volk et al., 1997).

20         $\chi_0(t') \, G(r,t') \, L(r,t')$ (1)

21   The source function, $\chi_0(t')$, is estimated to have a trend of about 3 %/decade from 1990 to 2003,

22   as discussed later in Sect. 5. The loss function at a given stratospheric location, $L(r,t')$, is related

23   to the decay of the tracer along the complete path spectrum (all pathways from the entrance

24   region, or tropical tropopause, to the specific location), and only tracers with constant

25   tropospheric values and of a radioactive decaying type within the stratosphere are truly path

26   independent (Hall and Plumb, 1994). Even if the time series for the CH_4 source gas is

27   approximately linear, it should be clear from Fig. 2 that $L(r,t')$ is spatially inhomogeneous in

28   both the vertical and meridional directions. Although one cannot easily sort out the effects of

changes in the mean age of air from changes in the path spectra for the BDC (Schoeberl et al.,

2000), trends from observed time series of CH_4 are considered as a function of latitude and

altitude in the present study. The tropospheric trends in the CH_4 source gas are small, and its

annually-averaged, chemical loss term in the stratosphere should give rise to spatial gradients

that are very nearly symmetric across the two hemispheres. Despite those considerations for

hemispheric symmetry, the analyses of time series of observed stratospheric CH_4 show that their

long-term trends differ between the northern and southern hemispheres and indicate significant

changes for the BDC in the middle stratosphere.

2 Objectives

The modeled CH_4 distribution in Fig. 2 is very similar to observed wintertime distributions of

CH_4 from satellite datasets. CH_4 is decreasing with pressure-altitude and with latitude because

CH_4 is oxidized in a multi-step process to H_2O in the middle and upper stratosphere (e.g.,

Brasseur and Solomon, 2005). In an early study using CH_4 data from the Stratospheric and

Mesospheric Sounder (SAMS) on Nimbus 7, Stanford and Ziemke (1991) determined

empirically that the minimum lifetime for its chemical conversion to H_2O is of the order of 3 to 4

months at low latitudes in the upper stratosphere or somewhat longer than the time constants for

the mean meridional transport. Holton and Choi (1988) and Stanford et al. (1993) used the three

years of SAMS CH_4 data as a tracer for the characterization of the vertical and meridional

components of the seasonal net transport. The present analysis study makes use of time series of

CH_4 mixing ratio data as a function of pressure-altitude for 1992-2005 from the Halogen

Occultation Experiment (HALOE) aboard the Upper Atmosphere Research Satellite (UARS).

As noted by Rosenlof (2002), atmospheric sampling via the method of solar occultation is

adequate typically for obtaining the large-scale variations of CH_4.

The HALOE instrument obtained sunrise (SR) and sunset (SS) profiles of CH_4 in the stratosphere

and lower mesosphere, and a number of researchers have made use of its CH_4 data for studies of

middle atmosphere transport. Ruth et al. (1997), Randel et al. (1998), Gray and Russell (1999),

5

1   Randel et al. (1999), and later Shu et al. (2013) used the multi-year distributions of the HALOE

2   CH_4 mixing ratio as a tracer for the effects of the semi-annual oscillation (SAO) and quasi-

3   biennial oscillation (QBO) forcings. Youn et al. (2006) analyzed time series of CH_4, H_2O, and

4   HF from HALOE for their trends at 10 hPa and in one latitude zone, 40 to 45 degrees, and they

5   found differences in their trends between the two hemispheres. They related the trends that they

6   found for the northern hemisphere to an intensification of stratospheric wave activity over that

7   14-yr time span.

8

9   The present study is an analysis of time series of the HALOE CH_4 for an increasing trend in the

10   tropical ascent and for a correspondingly increasing trend in the extratropical descent in the same

11   hemisphere. Multiple linear regression (MLR) techniques are used for the analyses and are

12   discussed in Section 3, and they fit the seasonal and the interannually-varying forcings along

13   with the trend terms in time series of CH_4 as a function of latitude and pressure-altitude.

14   Preliminary MLR model results are also shown in Sect. 3, and concerns about having an

15   adequate number of profile samples for each of the SR and SS crossings of a latitude zone are

16   addressed in Section 4. Final sets of CH_4 time series are selected as representative of the tropical

17   and extratropical latitude zones of each hemisphere, as depicted in the simple schematic of

18   Plumb (2007, his Fig. 13). An estimate of the trends for the CH_4 source gas is presented in

19   Section 5. Then the coefficients of the stratospheric trend terms from HALOE and their

20   statistical significance are given and compared with that of the source gas for each latitude zone

21   and as a function of pressure-altitude. Trends from the study herein are compared with those

22   reported by other groups, which in some instances were based only on data through the 1990s.

23

24   Trends from analyses of HALOE H_2O are shown in Section 6 and compared with those of CH_4

25   for consistency, since H_2O is the primary chemical product of CH_4 oxidation at the upper

26   altitudes. Section 6 also relates the time series of residuals from analyses of CH_4 in the lower

27   mesosphere to de-seasonalized variations in HCl, another molecule that contains information

28   about the BDC of the stratosphere and mesosphere. In particular, it is shown that the residuals

1   from the separate MLR fits to the CH_4 and HCl series have small, irregular variations of opposite

2   sign. It will be posited that the somewhat anomalous variations in the multi-year time series of

3   HALOE HCl for the lower mesosphere that have been reported by others are due to effects from

4   anomalous wave forcings during 1999-2002. Section 7 is a summary of findings from the

5   present analyses.

6

7   3 Analysis approach

8   Effects from the seasonal BDC are apparent from monthly, zonal-mean cross sections of CH_4, as

9   shown by Holton and Choi (1988) from the SAMS data and by Randel et al. (1998) and Shu et

10   al. (2013) from the HALOE data. Qualitatively, there is a net upward transport of CH_4 at the low

11   latitudes, a net poleward transport throughout the stratosphere, plus a descent of CH_4-poor air

12   within the polar vortex beginning at upper altitudes (cf., Fig. 2). The monthly CH_4 distributions

13   also exhibit a significant, negative mixing ratio gradient from the tropics to higher latitudes along

14   pressure surfaces in the middle and upper stratosphere. The exact latitude location of the

15   maximum gradient varies seasonally, according to the strength of the meridional mixing of the

16   air masses that occurred in the weeks before. Latitude versus pressure-altitude cross sections of

17   the CH_4 from the HALOE Website (http://haloe.gats-inc.com/home/) for October of successive

18   years reveal that the isolines of the tropical CH_4 distribution did not extend into the upper

19   stratosphere during 1991, 1993, 1995, 1997, 1999, and 2004, while they were elevated in 1992,

20   1994, 1998, 2002, and 2003. CH_4 variations for 1996, 2000, and 2001 were intermediate to

21   those of the other years. Gray and Russell (1999) and Shu et al. (2013) showed that the apparent

22   strength or upward extent of the CH_4 due to the mean meridional circulation is related to the

23   phase of the QBO and/or to the effects of the Rossby-wave forcing. To first order, the isolines of

24   the CH_4 in Fig. 2 and in the HALOE data also indicate that there are distinct BDC branches in

25   the northern hemisphere and in the southern hemisphere. The sense of that circulation is upward

26   in the tropics and subtropics and downward at the high latitudes.

27

1   Points for the data time series of the present study are generated using the HALOE version 19,

2   Level 2 CH_4 profiles from occurrences of the HALOE SR or SS tangent-point observations

3   within a latitude zone for 1992-2005, as in Remsberg (2008). The SR and SS profiles are binned

4   into 14 overlapping latitude zones from 65˚S to 65˚N and at 12 pressure-altitudes, giving a total

5   of 168 separate time series for analysis. Initially, the width of each latitude bin was set to 20

6   degrees, ensuring a relatively large number of samples. Example time series for the southern and

7   northern extratropics are shown in Fig. 3 at 10 hPa (near 31 km). Each data point in Fig. 3 is an

8   approximate snapshot of the zonally-averaged CH_4 for the latitude zone (cf., Fig. 2). The

9   oscillating curves in Fig. 3 are the MLR fits to the data points from mid-1992 onward and based

10   on the terms indicated at the lower left of the figure. The near horizontal line is the sum of the

11   constant and linear trend terms of the MLR model.

12

13   Results of similar MLR analyses of time series of HALOE data were reported for ozone

14   (Remsberg, 2008), temperature (Remsberg, 2009), and mesospheric water vapor (Remsberg,

15   2010). Details of the formulation of the terms for the MLR models can be found in Remsberg

16   (2008) and are summarized here. Initially, only semiannual (SAO) and annual (AO) terms are

17   considered for the model. A Fourier analysis is then applied to the residual or difference of the

18   model values from the points in the time series, in order to identify significant periodic,

19   interannual terms that remain. Three interannual terms are almost always present and are

20   included in the model: an 838-dy (27.5-mo) or QBO1 term; a small amplitude, 718-dy (23.5-

21   mo) biennial or QBO2 term; and a 690-dy (22.6-mo) sub-biennial (SB) term, whose period arises

22   from the difference interaction between QBO and annual terms. The relative amplitudes of these

23   three interannual terms vary with latitude and altitude. The 22.6-mo term agrees closely with the

24   anti-symmetric empirical orthogonal function (EOF) identified by Dunkerton (his Eq. (5.2),

25   2001) for the subtropical latitudes from a shorter series of HALOE CH_4 data. The primary

26   purpose of identifying and including interannual terms in the MLR model is so that their

27   significant structures can be accounted for. A linear trend term is also part of the final models.

28   Lag-1 autocorrelation (AR-1) effects are a significant part of the MLR models for zonally-

29   averaged stratospheric data. The accounting for AR-1 effects corrects for minor, but important

8

1   biases between the MLR model and the CH_4 points that often occur along short segments of the

2   data series. Corrections for AR-1 effects follow the two-step approach of Tiao et al. (their

3   Appendix A, 1990), and those corrections have a significant impact on the analyzed trend terms.

4

5   Data in the first year following the Mt. Pinatubo eruption of June 1991 often appear to have been

6   perturbed, so that time span is not considered for the MLR fittings. In Fig. 3 (bottom) one can

7   see that there is a weak, decadal-scale variation in the data series, whose amplitude is

8   characterized by a difference interaction between the QBO1 and SB terms (or a 10.6-yr period).

9   However, a separate term with that period is not part of the MLR models of the present study. In

10   addition, Nedoluha et al. (1998) reported that solar cycle (SC) effects on CH_4 are very small even

11   near the stratopause; thus, no 11-yr or SC-proxy term is included in the MLR models. However,

12   there is a cooling of the middle atmospheric during this 14-yr time span, due to the increasing

13   atmospheric CO_2. Therefore, the analyses are conducted for time series of the CH_4 mixing ratio

14   at pressure-altitudes rather than geometric altitudes. In this way, the added effects from the

15   contraction of a pressure surface with altitude and time are avoided. To first order then, the

16   variations of CH_4 with time at a pressure level represent the effects of the diabatic transport

17   vertically within a zone and any horizontal mixing to adjacent latitude regions.

18

19   Figure 3 depicts the time series for 10 hPa and at 55˚ latitude for the two hemispheres. Figure 4

20   shows the associated, annual mean distribution of CH_4 that is based on the constant terms from

21   the MLR models, and the mean mixing ratios for 10 hPa are also nearly the same or 0.77 ppmv

22   at 55˚N and 0.82 ppmv at 55˚S. The amplitudes of the SAO and the AO terms in Fig. 3 are more

23   distinct in the southern than in the northern hemisphere, despite the fact that the seasonal cycle

24   for the mean meridional circulation of each hemisphere is mainly just a response to very similar

25   changes in the differential heating between Equator and Pole. Figure 3 (bottom) shows that the

26   seasonal maximum occurs in late autumn to early winter in the northern extratropics, and its

27   minimum is in late summer. It may be that the SAO and AO cycles at 55˚N are influenced and

28   its annual mean mixing ratio reduced slightly, due to meridional mixing of the air during late

1   winter to spring. On the other hand, Fig. 3 (top) at 55˚S shows minimum data values of 0.5 to

2   0.6 ppmv for some years and most often in late winter, and they are not fit well by its MLR

3   model. That circumstance is because those perturbations in the CH_4 data occur for only a short

4   time (few weeks) in late winter/early spring, or at the time of the final warming in the southern

5   hemisphere; that rapid variation is not resolved by the terms of the MLR model. The amplitudes

6   of the several interannual terms are also significant in the extratropics at 10 hPa. Finally, the

7   trend coefficients from the data of Fig. 3 are slightly positive in the south but negative in the

8   north; that difference is discussed further in Sect. 5.

9

10   Corresponding CH_4 time series at 7 hPa are shown for the two subtropical zones in Fig. 5.

11   Periodic variations in Fig. 5 (top) for the southern hemisphere are primarily from the annual and

12   QBO cycles; its average CH_4 is about 1.1 ppmv. Effects from the SAO term do not emerge

13   clearly until the upper stratosphere (not shown). The data for the northern subtropics in Fig. 5

14   (bottom) indicate a seasonal cycle that is more variable and somewhat weaker than in the south;

15   interannual effects (QBO and SB) are present but are weaker, too. In general, there is less

16   periodic structure in the CH_4 of the northern subtropics at this level, again most likely because of

17   the mixing effects from the dissipation of Rossby waves and gravity waves. Mixing of air from

18   the middle latitudes may explain its occasional, low wintertime data values (e.g., Ploeger et al.,

19   2014). The trend coefficients are positive for the subtropics of both hemispheres. At this point it

20   is also noted that changes in the BDC based on the CH_4 variations in the southern subtropics can

21   also be affected by the stronger, extratropical wave forcings of the northern hemisphere (see also

22   Sect. 6).

23

24   Estimates of the trends for CH_4 in terms of latitude versus pressure-altitude are shown in Fig. 6.

25   In this case the HALOE CH_4 profiles are averaged for each of the 12 pressure-altitudes from 0.4

26   hPa to 50 hPa and within 14 overlapping, 20˚-wide latitude bins centered from 65˚S to 65˚N.

27   Trend contours are drawn at intervals of 4 %/decade; the solid contours are positive, while the

28   dashed contours are negative. Positive trends occur at low to middle latitudes and are interpreted

1 as indicating an upward acceleration for the tropical branch of the BDC plus an acceleration

2 poleward. The negative or dashed trends at the high latitudes indicate the downward

3 acceleration of the polar branch of the BDC within each hemisphere. Dark shading in Fig. 6 is

4 where the trend term from the MLR model is present with greater than 90% confidence; lighter

5 shading denotes where that confidence is between 70% and 90%. The trend profiles at most

6 latitudes from 50 hPa to about 5 hPa are significant and display a coherent character for an

7 acceleration of an Equator-to-Pole or BDC circulation within each hemisphere, at least during

8 the period of the HALOE measurements. The trends from 50 hPa to about 10 hPa are also

9 clearly asymmetric or positive in the northern hemisphere and near zero in the southern

10 hemisphere. However, the trends in the tropics are of the order of 3 %/decade or equivalent to

11 that expected from the tropospheric source gas (see also Sect. 5). Thus, the near zero trends at

12 15˚S to 35˚S indicate that the transport and mixing of low values of CH_4 may have been

13 increasing away from the edge of the southern winter polar vortex (55˚S to 65˚S), where the

14 trends are also near zero during 1992-2005.

15

16 **4 Data sampling and data bias concerns**

17 Figure 6 shows that there are rather sharp meridional gradients in the CH_4 trends of the upper

18 stratosphere at 35˚N, but not at 35˚S. The middle latitudes are where there is often a strong

19 negative meridional gradient in the isolines of CH_4 (c.f., Fig. 2), but the MLR models herein do

20 not have a term to account for a variation with latitude. Rosenlof (2002, her Fig. 4) did not find

21 a similar strong gradient in the trends from her analyses of HALOE profiles, but then she only

22 analyzed data for 1992-2001. Another important difference is that she averaged the HALOE

23 profiles within latitude bins of width 5˚, rather than 20˚. A narrower bin width is clearly

24 preferred, but there can be a problem with having fewer profiles for the latitude bin. This

25 concern is explored, as follows. First, it is noted that major advantages of solar occultation

26 measurements are the high signal-to-noise for their limb transmission profiles and their

27 inherently good vertical resolution; each retrieved HALOE CH_4 profile is quite accurate and has

28 a vertical resolution of about 4 km (Park et al., 1996). Still, for the lower latitudes HALOE

29 typically made its measurements across a given latitude bin over just a few days, due to the

11

1   alternating nature of the time sequence of its SR and SS occultations from the UARS satellite.

2   Rosenlof (2002) combined the SR and SS measurements within 5˚ bins and calculated their

3   monthly averages. However, in the present study the SR and SS profiles are averaged separately.

4   In addition, the exact latitude crossing times for their averages are retained, in order to yield

5   better fits for the AO and especially the SAO terms of the MLR model. A minimum of 5 profiles

6   is required for the separate SR or SS bin averages; that number is judged as representative of the

7   true zonal mean because the separation between profiles from successive orbits is about 24˚

8   longitude. The zonal wave amplitudes from the CH_4 are normally periodic and also have small

9   amplitudes compared with its zonal mean value. An exception is at high latitudes during

10   dynamically active winters, but those occurrences are rather short and infrequent across the 14-yr

11   time series of the HALOE measurements. Further, it is found that requiring a minimum of 7

12   profiles gives time series having slightly fewer data points, but their analyzed trends are

13   essentially the same as before.

14

15   To have separate SR and SS samples that are representative of zonal mean CH_4, a bin width of

16   10˚ is chosen for the data points of the time series, and final MLR analyses are carried out.

17   Table 1 compares the resulting trend profiles using bin widths of 10˚ versus 20˚ for three selected

18   latitudes of the northern hemisphere. The trend terms that are highly significant are in bold, i.e.,

19   having a confidence interval (CI) of being present in the time series that is greater than or equal

20   to 95%. Where the corresponding trends are significant at a given latitude, they are not changed

21   by much using the narrower bins. However, for the upper stratosphere of Table 1 at 35˚N, the

22   trends are smaller now compared with those found in Fig. 6 using the wider bins. Though not

23   highly significant, those changes are the result of including measured profiles that are more

24   nearly representative of the exact latitude zone of 35˚N. The previously large positive trends in

25   the upper stratosphere in Fig. 6 may imply that the location of a given isoline of CH_4 moves

26   poleward due to changes in the wave activity and mixing. No similar change is evident for the

27   middle latitudes of the southern hemisphere. An analysis of trends in the transport from an

28   assimilation model is required to really interpret those changes at 35˚ latitude because the present

29   results from HALOE CH_4 are truly due to the combined effects of the stratospheric age spectra,

12

G, and the loss function, L. The remainder of the paper focuses on trend results obtained from profiles in selected bins of 10˚ in width.

Changes in the HALOE instrument were evaluated in terms of any potential errors for the trends in the data over its 14-yr time series (Gordley et al., 2009). They found that there was a change in the CH_4 gas cell concentration, leading to a false trend in its CH_4 mixing ratio of -1.9±0.7 (1σ) %/decade that is constant with pressure-altitude. A first order correction for that false trend would be to add 1.9 %/decade to the analyzed trends, although that correction is not applied to the final results herein because it is not obtained strictly from the MLR fit process. A separate concern relates to the pressure profiles associated with the HALOE Level 2 CH_4 transmission signals. Specifically, an initial registration for the retrieval uses the temperature versus pressure or T(p) values at 31.5 km altitude from operational data that were supplied to the UARS Project in near real time by the NOAA Climate Prediction Center (CPC) (Thompson and Gordley, 2009). The Level 2 retrieval algorithm for T(p) also uses transmission measurements from the HALOE CO_2 channel that are accurate for the upper stratosphere. There is a weighted merger of the HALOE retrieved T(p) with the CPC profiles over the altitude range of 31.5 to 45 km, such that the final Level 2 T(p) profiles are principally those from the measurements of HALOE down to about the 4-hPa level. Remsberg and Deaver (2005, their Fig. 4) found a discontinuity near May 2001 in the HALOE T(p) times series for 5 hPa (near 36 km) at 10˚N but not at 3 hPa, and that shift is traceable to a change in the operational temperatures at that time. However, the retrieved CH_4 mixing ratio versus pressure profiles are in hydrostatic balance. No similar discontinuity is indicated in the time series of the HALOE CH_4 at 10 hPa (Fig. 3), at 7 hPa (Fig. 5), or at the other analyzed levels (not shown).

5 Trends in CH_4 from the troposphere and in the stratosphere

It is important to have a good estimate of the trends for the source term, χ_0, so that its effects can be separated from the product of expression (1), at least to first order. Because there is about a 1-yr delay for the surface methane source gas to reach the tropical middle stratosphere, a time

1   frame of 1991-2004 is considered for the time series of the source gas. Methane from remote

2   boundary layer sites was globally-averaged by Dlugokencky et al. (2001; 2009). They showed

3   that the de-seasonalized CH_4 mixing ratios continued to grow during this period, although at

4   rates that were slower from 1992 to 1999 (3.0 %/decade) and from 1999 to 2005 (near zero) than

5   from 1983 to 1992 (4.7 %/decade). Exceptions were the episodic increases in 1991 and 1998

6   that were followed by equally sharp decreases a year later. An overall trend of 3.0±0.7 %/decade

7   is obtained by considering the endpoint values at 1991 and 2004 from their globally-averaged

8   data time series. At the high latitudes the overall trend may be slightly larger because the age-of-

9   air is older there. Globally-averaged, 1-σ uncertainties from the station data are of the order of

10 0.6 ppbv/yr, giving the 2-σ value of 0.7 %/decade for the overall trend estimate.

11

12 A separate indication of trends from the CH_4 source term to the stratosphere is obtained for the

13 tropics from the MLR analyses of the HALOE data. Specifically, Fig. 7 shows CH_4 time series

14 at 50 hPa for 5˚S and 5˚N that are part of the trend results in Fig. 6. Their linear trends and 2σ

15 uncertainties are 2.8±2.8 and 3.3±3.4 %/decade, respectively, or essentially the same values as

16 from the tropospheric time series, although the tropospheric data have a much smaller

17 uncertainty. The two tropical time series in Fig. 7 have their maximum in late 1992 and a

18 somewhat non-linear (quadratic) character thereafter with a second maximum in 1999. Both

19 maxima follow the observed episodic increases in the troposphere by about a year. The average

20 HALOE trend (and 2σ) values are 1.7±2.1 and 3.1±2.1 %/decade at 30 hPa for 5˚S and 5˚N from

21 Fig. 6; however, the data time series at 30 hPa exhibit very little to no non-linear character (not

22 shown), and that is also the case at the other pressure-altitudes.

23

24 The retrieved HALOE CH_4 mixing ratios in Fig. 7 are only of order 1.4 ppmv in early 1992.

25 Such low values may indicate a slight bias error at 50 hPa, due to a reduced accuracy for the

26 measured and retrieved CH_4 in the presence of the aerosol layer following the eruption of Mt.

27 Pinatubo. However, Thomason (2012) reported that HALOE CH_4 does not appear to be affected

28 by contamination from other minor or trace species within its retrieval algorithm, at least after

29 that early volcanic period. The present study considers data points from mid-1992 and onward

1   for the MLR analyses at all latitudes and pressure-altitudes, primarily to avoid contaminating

2   effects in the lower stratosphere and/or anomalous net transport effects at higher altitudes for

3   some months following the eruption. There is also a small, but clear SR/SS bias in the data of

4   Fig. 7 that is not considered real. Most likely, that bias comes about because the temperature-

5   pressure-altitude data from the NOAA CPC that are used to register the HALOE Level 2 mixing

6   ratio profiles in the lower stratosphere. Those provisional data are for 12Z; they do not reflect

7   the effects of the diurnal tide on pressure that are significant in the tropics. No correction is

8   applied to the separate SR and SS time series before they are combined and analyzed, however.

9

10   Time series of CH_4, like those in Figs. 3 and 5, are analyzed at 60˚S, 35˚S, 10˚S, 10˚N, 35˚N, and

11   60˚N, and their latitude bins have a width of 10˚. Table 2 contains the mean CH_4 mixing ratio

12   profiles from the constant terms of the MLR models for each of the six latitude zones. The term

13   coefficients show very good symmetry between the two hemispheres in the tropics and at the

14   high latitudes. In the middle to lower stratosphere there is slightly more CH_4 in the southern than

15   in the northern high latitudes, indicating that the net wintertime descent is prolonged and/or a bit

16   stronger in the north. At 50 hPa the mixing ratios are very nearly identical between the two

17   hemispheres for the tropics (1.57 ppmv), middle latitudes (1.34 ppmv), and at high latitudes

18   (1.22 ppmv), indicating that the tropospheric CH_4 that entered the lowest part of tropical

19   stratosphere is being transported poleward and mixed about equally with the higher latitude air.

20   There is also a monotonic decrease of the CH_4 with altitude in each latitude zone, due to the

21   chemical oxidation of CH_4 to H_2O. The mean CH_4 mixing ratio profiles in Table 2 represent

22   qualitatively the effects of the seasonal BDC transport within each hemisphere.

23

24   The conceptual idea of Plumb (2007, his Figs. 13 and 15) is employed for the detection of an

25   acceleration of the hemispheric BDC using a species like CH_4, whose mixing ratio decreases

26   with altitude as in Figs. 2 and 4. Trends from the HALOE CH_4 time series are interpreted as

27   indicating a change in the strength of the BDC, when they are positive and significantly larger

28   than 3.0±0.7 %/decade in the tropics or significantly smaller or even negative at the high

1 latitudes. Thus, an acceleration of the BDC leads to higher CH_4 values in the tropics and lower

2 values in the extratropics or a steepening of its Equator-to-Pole gradient with time for a given

3 pressure-altitude. On the other hand, the effects of meridional mixing can transport extratropical

4 air back to the subtropics and cause a net recirculation and further aging of the CH_4 (Garny et al.,

5 2014). It is not possible to quantify those separate effects based on the CH_4 observations alone.

6 The analyzed trend terms (%/decade) and the accompanying confidence intervals or CI (in %)

7 for their presence in the time series are given in Table 3. The signs of the trend terms indicate

8 that there is an acceleration of the overall BDC within the middle stratosphere. Note that the

9 highly significant trends are shown by boldface type; they have a CI equal to or greater than 95%

10 of being present in the time series. The trend coefficients are highly significant and different

11 from the trend in χ_o in both the tropics and extratropics from 20 to 7 hPa of the northern

12 hemisphere but only in the tropics from 10 to 5 hPa for the southern hemisphere. It is noted that

13 some of the relatively large trends for the CH_4 time series at high latitudes of the upper

14 stratosphere also carry fairly small uncertainties from the MLR analyses, but those trends are not

15 considered significant because there is non-periodic structure in the time series of their residuals

16 that has not been accounted for.

17

18 Figure 8 is a plot of the trend profiles in %/decade from Table 3 for 10˚S and 60˚S or within the

19 tropical pipe region of the lower stratosphere and near the edge of the polar vortex region,

20 respectively. Their 2σ uncertainties are shown as horizontal bars at the tropical levels, where the

21 results are highly significant. Those trends are 17.4 (3.8) at 5 hPa, 13.3 (3.6) at 7 hPa, 6.9 (3.1)

22 at 10 hPa, and 1.8 (3.6) at 20 hPa. The vertical dashed line represents the trend of 3 (0.7)

23 %/decade, which is the estimate of that for the tropospheric CH_4. The trend at 5 hPa is large and

24 positive at 10˚S and negative at 60˚S, so at least their opposing signs are consistent with the

25 expectation for an acceleration of the BDC. The trends at 20 and 10 hPa are positive at both

26 latitudes, although they are less significant at 60˚S. On the other hand, there is no evidence for a

27 change of the shallow branch (70 to 30 hPa) of the BDC from these results. The CH_4 trend terms

28 near the stratopause are also insignificant.

29

1   Figure 9 is a plot of the trend profiles from Table 3 at 10˚N and 60˚N. The highly significant,

2   northern tropical trends and their 2σ uncertainties are 12.2 (3.4) at 7 hPa, 9.8 (3.2) at 10 hPa,

3   10.0 (3.2) at 20 hPa, 3.8 (4.2) at 30 hPa, and 3.3 (3.0) at 50 hPa. The significant trends for 60˚N

4   are -6.3 (20.4) at 5 hPa, -11.3 (14.4) at 7 hPa, -19.5 (9.0) at 10 hPa, and -8.4 (7.6) at 20 hPa.

5   Note that the foregoing trends are still significant after adding the first order correction of 1.9

6   %/decade for a change in the HALOE CH_4 gas cell. Trends at 50 hPa and 30 hPa vary from 3.3

7   to 3.8 %/decade at 10˚N and from 3.8 to 0.3 %/decade at 60˚N, but they carry the same sign and

8   disagree with the picture of an acceleration of the BDC. Yet, they are consistent with an average

9   trend of 3%/decade for the tropospheric CH_4, and they indicate that the trends at 60˚ latitude are

10   merely reflecting a net transport of tropical air to the higher latitudes. The CH_4 trends from 20

11   hPa to 7 hPa are larger and positive in the tropics, and the corresponding extratropical trends are

12   increasingly negatively up to 10 hPa and remain negative even at 5 hPa. Thus, the signs of the

13   trends from those two northern zones imply that there was an acceleration of the BDC in the

14   middle stratosphere during 1992 to 2005. In other words, an acceleration is indicated for the

15   lower part of the deep branch of the BDC.

16

17   Youn et al. (2006) obtained a positive linear trend at 10 hPa of 9 %/decade at 42.5˚S and almost

18   no trend at 42.5˚N. For comparison purposes, linear trends are calculated here for 10 hPa and for

19   the same narrow latitude zones of 40 to 45˚ in each hemisphere. Those trends are 5.7 (6.0) in the

20   southern and -4.6 (10.0) in the northern hemisphere. Possible reasons for the differing results

21   may be that the MLR model of the present study incorporates a larger number of periodic terms

22   plus the effects of autocorrelation among those terms. Coincidentally though, the trends shown

23   in Fig. 6 using the 20˚-wide latitude bins are 9.2 (3.0) at 45˚S and 0.0 (9.2) at 45˚N, which are

24   almost exactly the same values reported by Youn et al. (2006).

25

26   Changes for the BDC in the upper stratosphere are difficult to detect because the photochemical

27   lifetime for the conversion of CH_4 to H_2O is comparable to the time constant for the total

28   transport. The trend in Fig. 8 at 2 hPa is 5.0 (3.2) for 10˚S. The trend in Fig. 9 at the same level

1   is smaller and not significant for 10˚N or 1.2 (3.9). These findings are at odds with the rather

2   large decreasing trends for CH_4 at the lower latitudes in the upper stratosphere that were reported

3   earlier by Nedoluha et al. (1998, their Fig. 1) for the time span of 1991-1997, by Randel et al.

4   (1999, their Fig. 4) for 1992-1999, and even by Rosenlof (2002) for 1992-2001. An analysis of

5   the HALOE data is carried out for the latitude zone of 10˚S to 10˚N, but for the entire time

6   period of 1991-2005; the MLR fit to that particular time series is shown in Fig. 10.

7   Qualitatively, the structure in the time series data compares well with that of Nedoluha et al.

8   (1998) from late 1991 through early 1997, and separate analyses conducted here for that early

9   period also give large negative trends. Nevertheless, the trend at 2 hPa in Fig. 10 is weakly

10   positive or 3.1 %/decade and not significantly different from zero. Coincidentally though, that

11   small trend is consistent with what is estimated from the tropospheric CH_4 source gas data.

12

13   **6 Related trends for H_2O and HCl**

14   Supporting evidence is sought from the concurrent trends in HALOE H_2O because CH_4 is

15   oxidized chemically to H_2O in the upper stratosphere; their trends ought to be anti-correlated due

16   to that relationship (Brasseur and Solomon, 2005). The mean mixing ratio profiles for H_2O are

17   nearly symmetric for corresponding latitude zones of the two hemispheres (not shown). H_2O

18   values for the subtropics increase from about 3.9 ppmv at 50 hPa to about 6.3 ppmv at 0.5 hPa.

19   H_2O also increases slightly from the subtropics to the extratropics in the upper stratosphere, due

20   mostly to the oxidation of CH_4 to H_2O and to its subsequent transport poleward. Seasonal and

21   interannually-varying, entry-level values are found in the HALOE H_2O time series of the tropical

22   lower stratosphere. There is also an episodic decrease in those entry-level values in 2001

23   (Randel et al., 2006; Fueglistaler, 2012), although that change is nearly imperceptible at 10 hPa

24   in the time series of the middle latitudes. For the lower mesosphere it is presumed that changes

25   are small for the remaining part of the H_2O that are due to the variations of H_2O as it enters the

26   stratosphere through the tropical tropopause, or where the air has an average H_2O mixing ratio of

27   about 3.5 ppmv. Slightly less than half of the H_2O in the lower mesosphere is from the oxidation

28   of methane.

18

1

2   Trend profiles are obtained from HALOE H_2O using the same terms that were applied in the

3   MLR models for CH_4, and the results are shown and compared for 35°S in Fig. 11 and for 35°N

4   in Fig. 12. In order to get a better idea about their mutual changes, their trend profiles are plotted

5   in terms of ppmv/decade. Estimates of uncertainty are shown by the horizontal bars where the

6   trends are highly significant. The trend terms for H_2O in Fig. 11 are highly significant in the

7   lower stratosphere and also at 0.3 hPa. Trends for H_2O and CH_4 are of the same magnitude and

8   weakly positive in the upper stratosphere, but they are not highly significant. There are

9   indications of an anti-correlation in their mutual trends in Fig. 12 for the upper stratosphere of

10   the northern hemisphere that are more in keeping with that expected from the chemical oxidation

11   of CH_4 to H_2O. Their respective trends also have opposing signs in the lower stratosphere of the

12   northern hemisphere, but that finding is attributed to the trends for those two gases in their

13   tropical source region. In that regard, it is noted that the trend profiles for H_2O in Figs. 11 and

14   12 qualitatively support the modeled trend estimates of stratospheric H_2O for the longer time

15   span of 1986-2010 of Hegglin et al. (2014, their Fig. 5). Their modeled estimates also

16   considered observed trends in tropospheric CH_4 plus a chemical conversion to H_2O.

17

18   Figure 13 is the MLR model fit to the CH_4 time series data at 0.7 hPa of the northern extratropics

19   and subtropics. The minimum in the extratropics occurs in late summer, due to the nearly

20   complete oxidation of the CH_4 at that time. Conversely, there is a maximum in the subtropics in

21   late summer due to the upward diabatic circulation that is a dynamical response to the very warm

22   temperatures of the polar summer stratopause. Upon closer inspection, one can readily see that

23   these predominant, annual cycle variations in the data of the extratropics are different for some

24   years; those variations are underestimated by the MLR model terms in 1992 and from 2002-2005

25   and overestimated from 1999-2001. In the subtropics the late summer maximum is

26   overestimated by the model in 1996 and in 2000-2001. The model clearly underestimates the

27   subtropical data in the winter of 1997-98, too. Occasional, seasonal amplitude anomalies are

28   also present in the CH_4 analyses for the southern subtropics but are nearly absent in the southern

29   extratropics (not shown). It is likely that the more pronounced variations in the northern

19

hemisphere are related to the varying planetary wave activity and its effects on the mean meridional transport and mixing of the CH_4. Randel et al. (2000) reported that there was a minimum in the stratospheric wave forcing for the years 1993-1997, followed by an increase in 1998-1999. Pawson and Naujokat (1999) also noted that there were no midwinter warming events for the northern hemisphere in the middle 1990s. Manney et al. (2005) showed that they became more prevalent thereafter.

The seasonal terms of the MLR model simply provide an average fit to the data across all the years. Thus, the time series of HALOE CH_4 of the northern hemisphere indicate that there must be a connection to effects from aperiodic dynamical forcings. For example, the qualitative effect during and just following a warming event is to enhance meridional transport of a tracer (like CH_4) in the upper stratosphere and mesosphere. Hitchman and Leovy (1986) also found that there were secondary residual circulations in the subtropics associated with the descent of the SAO and also in response to stratospheric warming events. The MLR models do not account for the effects of such irregular forcings, and those unmodeled effects can affect the analyzed trends. Thus, it may be that those subtropical trends are merely reflecting the effects of changes in stratospheric wintertime warming activity during 1992-2005, rather than representing any longer-term trend for a change of the deep branch of the BDC at those upper levels. It ought to be possible to verify those instances of MLR/data mismatch with the aid of a model study for a CH_4-like tracer that is transported with the aid of assimilated temperature and ozone fields for those years in the manner of Ploeger et al. (2014).

A number of investigators have analyzed time series of HCl in the lower mesosphere to verify concurrent changes in the effects of reactive chlorine on ozone (e.g., Froidevaux et al., 2006). HCl is the primary product of the chemical conversion of free chlorine from methyl chloride and from CFC molecules in the upper stratosphere (Brasseur and Solomon, 2005). For this reason HCl may also be considered as a tracer-like species for studying transport and age-of-air, particularly for the uppermost stratosphere and lower mesosphere. Model studies show peak

1   values of HCl occurring in the lower mesosphere in 1999, while the HCl time series from

2   HALOE at 0.46 hPa and up to 2001 indicate that the observed maximum occurred a year of two

3   earlier or in 1997 (e.g., Waugh et al., 2001). However, the complete time series of HALOE HCl

4   shows two maxima—one in 1997 and another from 2001-2002 (WMO, 2007, Fig. 1-12). It may

5   be that there were significant variations in the observed HCl due to dynamical forcings at those

6   altitudes and that the chemical/transport models do not represent them so well. When the time

7   series of HALOE HCl are referenced to surfaces of constant CH_4, there is better agreement with

8   the modeled trends for HCl in terms of the known changes in its primary surface source gases or

9   CFCs (James Russell III and John Anderson, Hampton University, private communication,

10   2002). Thus, it appears that HALOE CH_4 represents a very effective tracer even in the lower

11   mesosphere, even though its mixing ratio there is small.

12

13   Spatial gradients for CH_4 and HCl in the lower mesosphere are opposite in sign both vertically

14   and in the meridional direction, such that any anomalies in their respective residuals should have

15   opposing features that would tend to confirm effects from dynamical forcings. Therefore, MLR

16   analyses are applied to time series of both CH_4 and HCl in the lower mesosphere. As shown in

17   Fig. 13, CH_4 has seasonal and QBO-like forcings that are resolved and accounted for reasonably

18   well with the MLR models; the same terms are applied to the HALOE HCl time series. A

19   quadratic term is also added to the linear term for its MLR model because HCl varies non-

20   linearly from 1992-2005. At $55\pm10°N$ and 0.7 hPa (near 52 km) the mixing ratio of HCl

21   increases from 2.6 ppbv in 1992 to a maximum of 3.6 ppbv in 2001 and then declines to an

22   average of 3.1 ppbv in 2005; CH_4 at 0.7 hPa is nearly constant or 0.2 ppmv over that time span.

23

24   Figure 14 (top) shows the time series of the residuals for HCl for 55°N and at 0.7 hPa. The

25   residuals (or data minus MLR model curve values) are obtained in this case by setting the AR-1

26   coefficient to zero, giving a better idea of anomalies for the modeled results. In general, the HCl

27   residuals indicate a good fit to the data, varying between ±0.2 ppbv or within 6% of the mean for

28   the data. Note though that the residuals are mostly negative in 1998 and 1999 and mostly

1 positive in 1995-1996 and in 2001-2002. Figure 14 (bottom) shows the corresponding residuals

2 for CH_4 that are of the order of ± 0.05 ppmv or about 25% of its mean value; those residuals

3 indicate little to no bias with the model from 1992 to mid-1999, but then show a clear negative

4 bias in 2000 and 2001, or opposite to that from HCl. Thus, there is aperiodic structure remaining

5 in the residuals for both HCl and CH_4, and their opposing signs during some years indicate that a

6 net transport may have been induced by the effects of wave forcings during those winters having

7 significant stratospheric warming activity. Recently though, Damiani et al. (2014) reported that

8 there can also be a chemical re-partitioning of HCl to $ClONO_2$ in response to a lower

9 mesospheric cooling following stratospheric warming events. The absence of any clear anti-

10 correlation between the HCl and CH_4 residuals of Fig. 14 for 1998-1999 indicates that HCl is not

11 strictly a passive tracer at that time but may be depleted slightly by the chemical repartitioning.

12 That prospect might also explain the small, but anomalous decrease in the HALOE HCl trends of

13 1998-1999 that were reported in WMO (2007).

14

15 **7 Conclusions**

16 Time series of the tracer-like molecule CH_4 obtained with the UARS HALOE experiment are

17 analyzed using MLR techniques for their periodic and trend terms during 1992-2005. The sunset

18 and sunrise profile data are binned according to tropical and high latitude zones of both the

19 southern and northern hemispheres. Time series are generated and analyzed from 50 hPa to 0.4

20 hPa. Based on an examination of the data time series, both seasonal and interannual terms are

21 included in the MLR models, in addition to a linear trend term. The trend terms are examined to

22 see whether there is any change in the BDC for the southern or northern hemispheres during

23 1992-2005 in accordance with the simple concept of Plumb (2007) for a hemispheric BDC. The

24 adoption of that approach indicates that an acceleration of the BDC can be detected where the

25 CH_4 trends are positive by more than 3%/decade in the tropics and less than that or negative at

26 the high latitudes. Further, since the analyses are conducted at pressure levels rather than at

27 geometric altitudes, it is presumed that any significant trends must be due mainly to changes

28 from the effects of wave forcings on the distributions of CH_4.

1

2   The primary findings of this study are as follows. The CH_4 trend terms for the northern

3   hemisphere are significant and positive from 50 hPa to 7 hPa at 10˚N and larger than the

4   tropospheric CH_4 trends of about 3 %/decade from 20 hPa to 7 hPa. At 60˚N the trends are

5   clearly negative from 20 hPa to 7 hPa. Thus, the overall trend signature across those two zones

6   indicates an acceleration of the BDC in the middle stratosphere of the northern hemisphere. The

7   CH_4 trends are positive and significant from 10 hPa to 5 hPa for 10˚S, and the corresponding

8   trends are negative at 7 hPa and 5 hPa for 60˚S but not highly significant; their combined trends

9   do not indicate an acceleration of the BDC for the southern hemispheric. The CH_4 trends are

10   also not highly significant for the stratosphere above the 5-hPa level in either hemisphere. The

11   early climate model simulations of Rind et al. (1990) are qualitatively consistent with these

12   findings, in that their model runs show more wave activity and dissipation throughout the winter

13   in the northern than in the southern hemisphere for their model scenario of steady increases of

14   CO_2 in the atmosphere. Still, it may be that these findings of a change in the BDC based on the

15   HALOE CH_4 are only representative of 1992-2005.

16

17   The trends for HALOE H_2O are compared at 35˚ latitude with those from CH_4 in the upper

18   stratosphere and lower mesosphere because H_2O is the primary product of the oxidation of CH_4

19   at those altitudes. An approximate inverse relationship between their trends is found in the

20   middle and upper stratosphere of the northern hemisphere, but not in the southern hemisphere.

21   The two gases show inverse trends in the lower stratosphere, too. However, while the trends for

22   HALOE H_2O are large and significant in the lower stratosphere, they reflect mostly the episodic

23   decrease for the entry-level H_2O to the stratosphere from below in 2001.

24

25   The variation of CH_4 with time in the lower mesosphere also provides some clues about the

26   effects of aperiodic wave forcings in that region. Other researchers have also reported that there

27   are modest disagreements in the modeled trends for HCl compared to those observed with

28   HALOE, particularly from about 1996 to 2002. Both CH_4 and HCl should serve as tracers of

1   any changes due to the wave forcings. In most instances their respective time series residuals are

2   anti-correlated and support the idea of a dynamical response to the wave activity. The observed,

3   small reductions of the HCl in the lower mesosphere for 1998-1999, however, do not seem to be

4   related to a corresponding increase in the CH_4 residuals. A chemical re-partitioning of HCl to

5   $ClONO_2$ may have occurred at that time. In summary, it is concluded that near-global

6   distributions of CH_4, as remotely measured from a satellite, are an excellent diagnostic of the

7   effects of seasonal and longer-term changes for the total transport within the middle atmosphere.

8

15

References

Andrews, D. G., Holton, J. R., and Leovy, C. B.: Middle atmosphere dynamics, Academic Press, Inc., Orlando, Florida, 489 pp., 1987.

Birner, T., and Bönisch, H.: Residual circulation trajectories and transit times into the extratropical lowermost stratosphere, Atmos. Chem. Phys., 11, 817-827, 2011.

Brasseur, G., and Solomon, S.: Aeronomy of the middle atmosphere, 3rd Edition, in Atmospheric and Oceanographic Sciences Library, vol. 32, Springer, The Netherlands, 644 pp., 2005.

Butchart, N.: The Brewer-Dobson circulation, Rev. Geophys., 52, 157-184, 2014.

Damiani, A., Funke, B., Lopez-Puertas, M., Gardini, A., von Clarmann, T., Santee, M. L., Froidevaux, L., and Cordero, R. R.: Changes in the composition of the northern polar upper stratosphere in February 2009 after a sudden stratospheric warming, J. Geophys. Res., 119, doi:10.1002/2014JD021698, 2014.

Dlugokencky, E. J., Bruhwiler, L., White, J. W. C., Emmons, L. K., Novelli, P. C., Montzka, S. A., Masarie, K. A., Lang, P. M., Crotwell, A. M., Miller, J. B., and Gatti, L. V.: Observational constraints on recent increases in the atmospheric CH_4 burden, Geophys. Res. Lett., 36, L18803, doi:10.1029/2009GL039780, 2009.

1   Dlugokencky, E. J., Walter, B. P., Masarie, K. A., Lang, P. M., and Kasischke, E. S.:

2   Measurements of an anomalous global methane increase during 1998, Geophys. Res. Lett., 28,

3   no. 3, 499-502, 2001.

4

5   Dunkerton, T. J.: On the mean meridional mass motions of the stratosphere and mesosphere, J.

6   Atmos. Sci., 35, 2325-2333, 1978.

7

8   Dunkerton, T. J.: Quasi-biennial and subbiennial variations of stratospheric trace constituents

9   derived from HALOE observations, J. Atmos. Sci., 58, 7-25, 2001.

10

11 Fleming, E.L., Jackman, C. H., Stolarski, R. S., and Considine, D. B.: Simulation of stratospheric

12 tracers using an improved empirically based two-dimensional model transport formulation, J.

13 Geophys. Res., 104, 23911-23934, 1999.

14

15 Froidevaux, L., Livesey, N. J., Read, W. G., Salawitch, R. J., Waters, J. W., Brouin, B.,

16 MacKenzie, I. A., Pumphrey, H. C., Bernath, P., Boone, C., Nassar, R., Montzka, S., Elkins, J.,

17 Cunnold, D., and Waugh, D.: Temporal decrease in upper atmospheric chlorine, Geophys. Res.

18 Lett., 33, L23812, doi:10.1029/2006GL027600, 2006.

19

20 Fueglistaler, S.: Stepwise changes in stratospheric water vapor?, J. Geophys. Res., 117, D13302,

21 doi:10.1029/2012JD017582, 2012.

22

23 Garcia, R. R, Randel, W. J., and Kinnison, D. E.: On the determination of age of air trends from

24 atmospheric trace species, J. Atmos. Sci., 68, 139-154, doi:10.1175/2010JAS3527.1, 2011.

1

Garny, H., Birner, T., Boenisch, H., and Bunzel, F.: The effects of mixing on age of air, J. Geophys. Res., 119, doi:10.1002/2013JD021417, 2014.

Gordley, L. L., Thompson, E., McHugh, M., Remsberg, E., Russell III, J., and Magill, B.: Accuracy of atmospheric trends inferred from the halogen occultation experiment, J. Appl. Remote Sensing, 3, 033526, doi:10.1117/1.3131722, 2009.

Gray, L. J., and Russell III, J. M.: Interannual variability of trace gases in the subtropical winter stratosphere, J. Atmos. Sci., 56, 977-993, 1999.

Hall, T. M., and Plumb, R. A.: Age as a diagnostic of stratospheric transport, J. Geophys. Res., 99, D1, 1059-1070, 1994.

Haynes, P. H., Marks, C. J., McIntyre, M. E., Shepherd, T. G., and Shine, K. P.: On the "downward control" of extratropical diabatic circulations by eddy-induced mean zonal forces, J. Atmos. Sci., 48, 651-678, 1991.

Hegglin, M. I., Plummer, D. A., Shepherd, T. G., Scinocca, J. F., Anderson, J., Froidevaux, L., Funke, B., Hurst, D., Rozanov, A., Urban, J., von Clarmann, T., Walker, K. A., Wang, H. J., Tegtmeier, S., and Weigel, K.: Vertical structure of stratospheric water vapour trends derived from merged satellite data, Nature Geoscience, 7, 768-776, doi:10.1038/ngeo2236, 2014.

Hitchman, M. H., and Leovy, C. B.: Evolution of the zonal mean state in the equatorial middle atmosphere during October 1978-May 1979, J. Atmos. Sci., 43, 3159-3176, 1986.

Holton, J. R.: Meridional distribution of stratospheric trace constituents, J. Atmos. Sci., 43, 1238-1242, 1986.

Holton, J. R., and Choi, W-K.: Transport circulation deduced from SAMS trace species data, J. Atmos. Sci., 45, 1929-1939, 1988.

Lin, P., and Fu, Q.: Changes in various branches of the Brewer-Dobson circulation from an ensemble of chemistry climate models, J. Geophys. Res., 118, 73-84, doi:10.1029/2012JD018813, 2013.

Manney, G. L., Zurek, R. W., O'Neill, A., and Swinbank, R.: On the motion of air through the stratospheric polar vortex, J. Atmos. Sci., 51, 2973-2994, 1994.

Manney, G. L., Krüger, K., Sabutis, J. L., Sena, S. A., and Pawson, S.: The remarkable 2003-2004 winter and other recent warm winters in the Arctic stratosphere since the late 1990s, J. Geophys. Res., 110, doi:10.1029/2004JD005367, 2005.

Nedoluha, G. E., Siskind, D. E., Bacmeister, J. T., Bevilacqua, R. M., and Russell III, J. M.: Changes in upper stratospheric CH_4 and NO_2 as measured by HALOE and implications for changes in transport, Geophys. Res. Lett., 35, 987-990, 1998.

Okamoto, K., Sato, K., and Akiyoshi, H.: A study on the formation and trend of the Brewer-Dobson circulation, J. Geophys. Res., 116, D10117, doi:10.1029/2010JD014953, 2011.

Park, J. H., Russell III, J. M., Gordley, L. L., Drayson, S. R., Benner, D. C., McInerney, J. M., Gunson, M. R., Toon, G. C., Sen, B., Blavier, J-F., Webster, C. R., Zipf, E. C., Erdman, P., Schmidt, U., and Schiller, C.: Validation of halogen occultation experiment CH_4 measurements from the UARS, J. Geophys., Res., 101, D6, 10,183-10,203, 1996.

Pawson, S., and Naujokat, B.: The cold winters of the middle 1990s in the northern lower stratosphere, J. Geophys. Res., 104 (D12), 14,209-14,222, 1999.

Ploeger, F., Riese, M., Haenel, F., Konopka, P., Müller, R., and Stiller, G.: Variability of stratospheric mean age of air and of the local effects of residual circulation and eddy mixing, J. Geophys. Res., doi:10.1002/2014JD022468, 2014.

Plumb, R. A.: Tracer interrelationships in the stratosphere, Rev. Geophys., 45, RG4005, doi:10.1029/2005RG000179, 2007.

Plumb, R. A., and Ko, M. K. W.: Interrelationships between mixing ratios of long-lived stratospheric constituents, J. Geophys. Res., 97, 10145-10156, 1992.

Randel, W. J., Wu, F., Russell III, J. M., Roche, A., and Waters, J. W.: Seasonal cycles and QBO variations in stratospheric CH_4 and H_2O observed in UARS HALOE data, J. Atmos. Sci., 55, 163-185, 1998.

1

2　Randel, W. J., Wu, F., Russell, III, J. M., and Waters, J.: Space-time patterns of trends in

3　stratospheric constituents derived from UARS measurements, J. Geophys. Res., 104, D3, 3711-

4　3727, 1999.

5

6　Randel, W. J., Wu, F., Russell III, J. M., Zawodny, J. M., and Nash, J.: Interannual changes in

7　stratospheric constituents and global circulation derived from satellite data, in Atmospheric

8　Science Across the Stratopause, (Siskind, D. E.; Eckermann, S. D., and Summers, M. E., Eds.),

9　American Geophysical Union, Washington, D. C., doi:10.1029/GM123p0271, 271-285, 2000,

10

11　Randel, W. J., Wu, F., Voemel, H., Nedoluha, G. E., and Forster, P.: Decreases in stratospheric

12　water vapor after 2001: links to changes in the tropical tropopause and the Brewer-Dobson

13　circulation, J. Geophys. Res., 111, D12312, doi:10.1029/2005JD006744, 2006.

14

15　Ray, E. A., Moore, F. L, Rosenlof, K. H., Davis, S. M., Sweeney, C., Tans, P., Wang, T., Elkins,

16　J. W., Bönisch, H., Engel, A., Sugawara, S., Nakazawa, T., and Aoki, S.: Improving

17　stratospheric transport trend analysis based on SF_6 and CO_2 measurements, J. Geophys. Res.,

18　119, doi:10.1002/2014JD021802, 2014.

19

20　Remsberg, E.: Observed seasonal to decadal scale responses in mesospheric water vapor, J.

21　Geophys. Res., 115, D06306, doi:10.1029/2009JD012904, 2010.

22

23　Remsberg, E. E.: Trends and solar cycle effects in temperature versus altitude from the halogen

24　occultation experiment for the mesosphere and upper stratosphere, J. Geophys. Res., 114,

25　D12303, doi:10.1029/2009JD011897, 2009.

1

Remsberg, E. E.: On the response of Halogen Occultation Experiment (HALOE) stratospheric

ozone and temperature to the 11-yr solar cycle forcing, J. Geophys. Res., 113, D22304,

doi:10.1029/2008JD010189, 2008.

5

Remsberg, E. E., and Deaver, L. E.: Interannual, solar cycle, and trend terms in middle

atmospheric temperature time series from HALOE, J. Geophys. Res., 110, D06106,

doi:10.1029/2004JD004905, 2005.

9

Rind, D., Suozzo, R., Balachandran, N. K., and Prather, M. J.: Climate changes and the middle

atmosphere. Part I: the doubled CO_2 climate, J. Atmos. Sci., 47, 475-494, 1990.

12

Rosenlof, K. H.: Transport changes inferred from HALOE water and methane measurements, J.

Meteorol. Soc. Japan, 80, 4B, 831-848, 2002.

15

Ruth, S., Kennaugh, R., Gray, L. J., and Russell III, J. M.: Seasonal, semiannual, and interannual

variability seen in measurements of methane made by the UARS Halogen Occultation

Experiment, J. Geophys. Res., 102, D13, 16189-16199, 1997.

19

Scherer, M., Voemel, H., Fueglistaler, S., Oltmans, S. J., and Staehelin, J.: Trends and variability

of midlatitude stratospheric water vapour deduced from the re-evaluated Boulder balloon series

and HALOE, Atmos. Chem. Phys., 8, 1391–1402, 2008.

23

Schoeberl, M. R., Sparling, L. C., Jackman, C. H., and Fleming, E. L.: A Lagrangian view of stratospheric trace gas distributions, J. Geophys. Res., 105, D1, 1537-1552, 2000.

Shaw, T. A., and Shepherd, T. G.: Raising the roof, Nature Geoscience, 1, 12-13, 2008.

Shepherd, T. G.: Transport in the middle atmosphere, J. Meteorol. Soc. Japan, 85B, 165-191, 2007.

Shu, J., Tian, W., Hu, D., Zhang, J., Shang, L., Tian, H., and Xie, F.: Effects of the quasi-biennial oscillation and stratospheric semiannual oscillation on tracer transport in the upper stratosphere, J. Atmos. Sci., 70, doi:10.1175/JAS-D-12-053.1, 2013.

Solomon, S., Kiehl, J. T., Garcia, R. R., and Grose, W.: Tracer transport by the diabatic circulation deduced from satellite observations, J. Atmos. Sci., 43, 1603-1617, 1986.

Stanford, J. L., and Ziemke, J. R.: CH_4 and N_2O photochemical lifetimes in the upper stratosphere: in situ estimates using SAMS data, Geophys. Res. Lett., 18, 677-680, 1991.

Stanford, J. L., Ziemke, J. R., and Gao, S. Y.: Stratospheric circulation features deduced from SAMS constituent data, J. Atmos. Sci., 50, 226-246, 1993.

Thomason, L. W.: Toward a combined SAGE II-HALOE aerosol climatology: an evaluation of HALOE version 19 stratospheric aerosol extinction coefficient observations, Atmos. Chem. Phys., 12, 8177-8188, 2012.

1

Thompson, R. E., and Gordley, L. L.: Retrieval algorithms for the halogen occultation

experiment, NASA/CR-2009-215761, available at http://www.sti.nasa.gov, 2009.

4

Tiao, G. C., Reinsel, G. C., Xu, D., Pedrick, J. H., Zhu, X., Miller, A. J., DeLuisi, J. J., Mateer,

C. L., and Wuebbles, D. J.: Effects of autocorrelation and temporal sampling schemes on

estimates of trend and spatial correlation, J. Geophys. Res., 95, 20,507-20,517,

doi:10.1029/JD095iD12p20507, 1990.

9

Volk, C. M., Elkins, J. W., Fahey, D. W., Dutton, G. S., Gilligan, J. M., Loewenstein, M.,

Podolske, J. R., Chan, K. R., and Gunson, M. R.: Evaluation of source gas lifetimes from

stratospheric observations, J. Geophys. Res., 102, D21, 25,543-25,564, 1997.

13

Waugh, D. W., Considine, D. B., and Fleming, E. L.: Is upper stratospheric chlorine decreasing

as expected?, Geophys. Res., Lett., 28, 1187-1190, 2001.

16

World Meteorological Organization: Scientific assessment of ozone depletion: 2006, Global

Ozone Research and Monitoring Project, Report No. 50, Geneva, Switzerland, 2007.

19

Youn, D., Choi, W., Lee, H., and Wuebbles, D. J.: Interhemispheric differences in changes of

long-lived tracers in the middle stratosphere over the last decade, Geophys. Res. Lett., 33,

L03807, doi:10.1029/2005GL024274, 2006.

23

Table 1. Methane trend profiles (%/decade). Bold denotes trend terms having confidence
intervals (CI) $\geq$ 95%.

P (hPa)	10N ±10	10N ±5	35N ±10	35N ±5	60N ±10	60N ±5
0.4	10.2	7.7	23.5	12.3	-8.5	-29.6
0.5	9.6	8.7	24.9	8.6	-10.7	-25.2
0.7	3.1	1.5	23.8	4.5	-17.8	-28.0
1.0	-0.6	-4.2	21.3	2.0	-19.0	-22.5
2.0	5.1	1.2	23.4	7.8	**-10.3**	-3.7
3.0	8.2	8.7	25.4	15.5	-7.2	-3.3
5.0	16.3	20.4	**15.7**	13.8	**-8.3**	**-6.3**
7.0	**11.5**	**12.2**	7.7	7.0	**-14.2**	**-11.3**
10.0	**7.4**	**9.8**	4.2	1.3	**-21.3**	**-19.5**
20.0	**8.0**	**10.0**	9.7	5.7	**-6.7**	**-8.4**
30.0	**4.3**	**3.8**	**10.7**	**8.6**	0.9	0.3
50.0	**3.4**	**3.3**	**6.5**	**6.2**	**3.4**	3.8

1   Table 2. Mean CH_4 mixing ratio profiles (ppmv).

P (hPa)	60S	35S	10S	10N	35N	60N
0.4	0.20	0.23	0.23	0.24	0.24	0.20
0.5	0.21	0.24	0.25	0.26	0.26	0.20
0.7	0.22	0.28	0.29	0.31	0.30	0.22
1.0	0.23	0.31	0.36	0.40	0.36	0.26
2.0	0.28	0.44	0.57	0.62	0.49	0.35
3.0	0.37	0.56	0.73	0.77	0.56	0.41
5.0	0.53	0.74	0.95	0.96	0.68	0.52
7.0	0.65	0.86	1.11	1.11	0.79	0.63
10.0	0.78	0.98	1.26	1.24	0.90	0.75
20.0	0.98	1.15	1.45	1.42	1.09	0.97
30.0	1.10	1.22	1.52	1.51	1.19	1.06
50.0	1.23	1.35	1.58	1.56	1.34	1.21

2

3

1   Table 3. Southern and northern hemisphere tropical and extratropical CH4 trend profiles (%

2   decade^{-1}) and their associated confidence intervals (CI in %) for the presence of the terms in the

3   MLR models.

4

Pressure (hPa)	60±5˚S, CI	10±5˚S, CI	10±5˚N, CI	60±5˚N, CI
0.4	-5.3, 75	8.6, 5	7.7, 34	**-29.6, 98**
0.5	-7.2, 72	9.4, 7	8.7, 33	-25.2, 93
0.7	-11.0, 83	11.0, 13	1.5, 18	-28.0, 92
1.0	-13.3, 89	5.9, 13	-4.2, 59	-22.5, 78
2.0	-6.2, 60	5.0, 21	1.2, 67	-3.7, 22
3.0	-5.4, 82	15.4, 48	8.7, 11	-3.3, 71
5.0	-3.7, 90	**17.4, 97**	20.4, 91	**-6.3, 99**
7.0	-0.7, 57	**13.3, 99**	**12.2, 97**	**-11.3, 99**
10.0	1.0, 7	**6.9, 96**	**9.8, 99**	**-19.5, 99**
20.0	4.0, 69	1.8, 93	**10.0, 99**	**-8.4, 97**
30.0	0.1, 7	1.5, 85	**3.8, 99**	0.3, 2
50.0	-4.1, 62	1.8, 70	**3.3, 99**	3.8, 84

5

6

7

Figure legends

1. Brewer-Dobson circulation (BDC) and stratospheric ozone. The sense of this net circulation or BDC is shown by the black arrows overlain on the zonally-averaged ozone distribution (or its number density in molecules per cm^3 versus latitude and altitude) for March 2004, as measured by the OSIRIS satellite instrument. Wiggly orange arrow indicates the propagation of waves from the troposphere as they affect the ozone. The dashed black line is the tropopause (adaption of figure in Shaw and Shepherd, 2008).


2. Methane distribution (ppmv) for January based on a chemistry and transport model simulation. White arrows indicate the sense and strength of the net circulation (image courtesy of Eric Fleming).

3. Time series of CH$_4$ is from HALOE at 10 hPa and at 55˚ latitude for the (top) southern and for the (bottom) northern hemisphere. Solid and open circles indicate the bin-averaged CH$_4$ data for sunset and sunrise, respectively. The oscillating curve is the MLR fit to the data based on the terms indicated at the lower left, and the near-horizontal line represents the sum of the constant and linear trend terms.

4. Annually-averaged, zonal mean HALOE methane from the MLR analyses (contour interval is 0.2 ppmv).

5. As in Fig. 3, but at 7 hPa and at 15˚ latitude for the (top) southern and for the (bottom) northern hemisphere.

6. Linear trends for HALOE methane (in %/decade). Zero and positive trends are solid contours and negative trends are dashed; contour interval is 4 %/decade. Dark shading denotes where the trends have a confidence interval (CI) $\geq$ 90%, and lighter shading denotes 70% $\leq$ CI $\leq$ 90%.

7. As in Fig. 3, but at 50 hPa and at 5° latitude for the (top) southern and for the (bottom) northern hemisphere.

8. Tropical and high latitude trend profiles for CH_4 in the southern hemisphere. Vertical dashed line is the approximate trend for tropospheric CH_4 or 3.0±0.7 %/decade. Horizontal bars show the 2σ error estimates for the highly significant trend terms.

9. As in Fig. 8, but for the northern hemisphere.

10. Time series of HALOE CH_4 at 2 hPa at the tropical latitudes for comparison with that of Nedoluha et al. (1998).

11. Trend profiles (in ppmv/decade) for CH_4 and H_2O at 35° latitude in the southern hemisphere. Horizontal bars denote the 2σ uncertainties for the highly significant trends.

12. As in Fig. 11, but for 35° latitude in the northern hemisphere.

13. As in Fig. 3, but for CH_4 at 0.7 hPa and at the latitudes of 55° (top) and 15° (bottom) of the northern hemisphere.

1   14. (top) Time series of HCl residual (data – MLR curve) at 0.7 hPa and at 55˚N; (bottom) time

2   series of CH_4 residual at 55˚N.

3

4
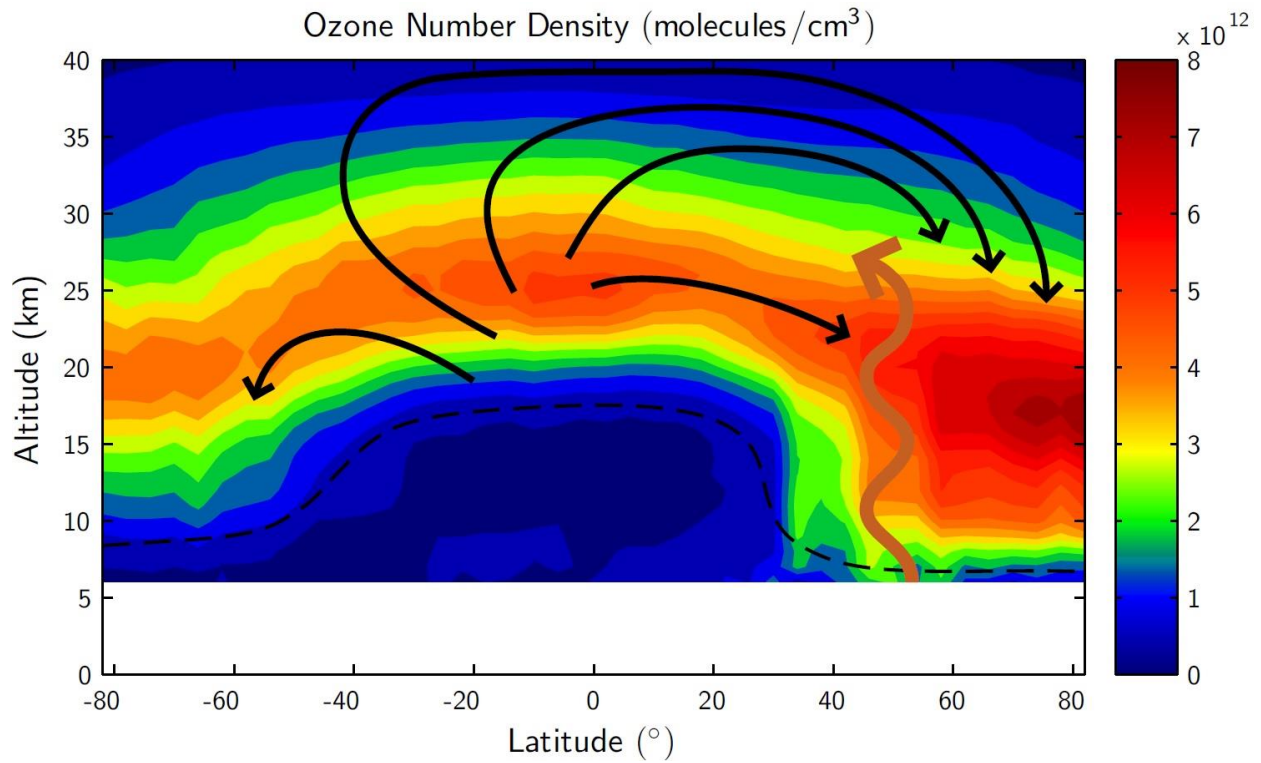
Figure 1. Brewer-Dobson circulation (BDC) and stratospheric ozone. The sense of this net circulation or BDC is shown by the black arrows overlain on the zonally-averaged ozone distribution (or its number density in molecules per cm^3 versus latitude and altitude) for March 2004, as measured by the OSIRIS satellite instrument. Wiggly orange arrow indicates the propagation of waves from the troposphere as they affect the ozone. The dashed black line is the tropopause (adaption of figure in Shaw and Shepherd, 2008).
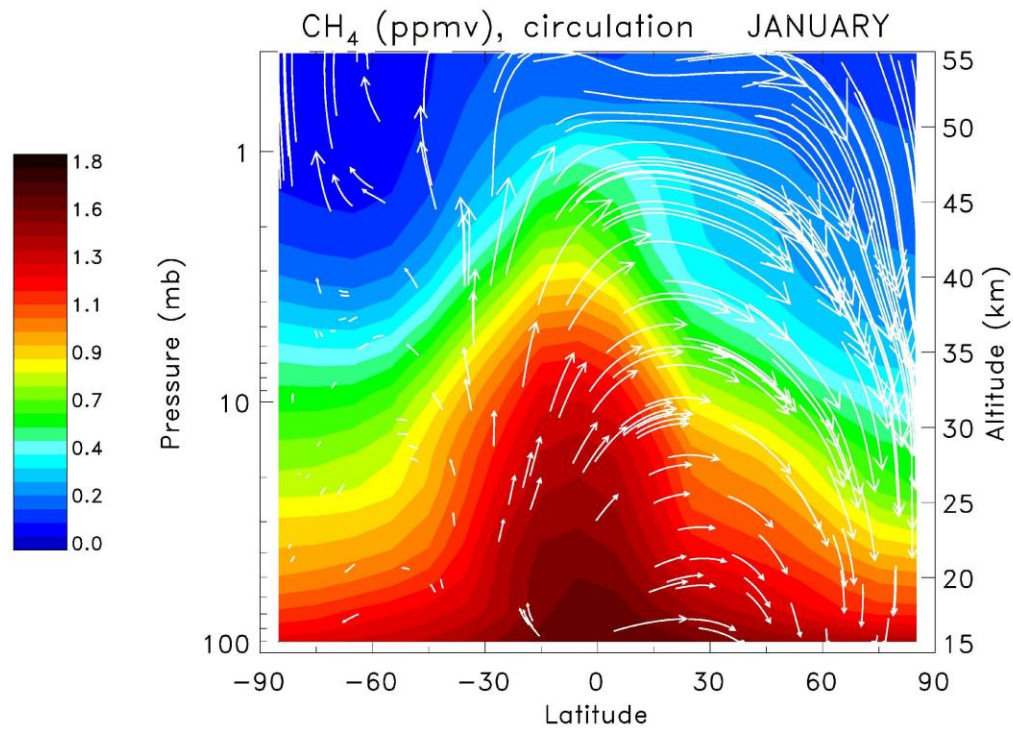
Figure 2. Methane distribution (ppmv) for January based on a chemistry and transport model simulation. White arrows indicate the sense and strength of the net circulation (image courtesy of Eric Fleming).

1
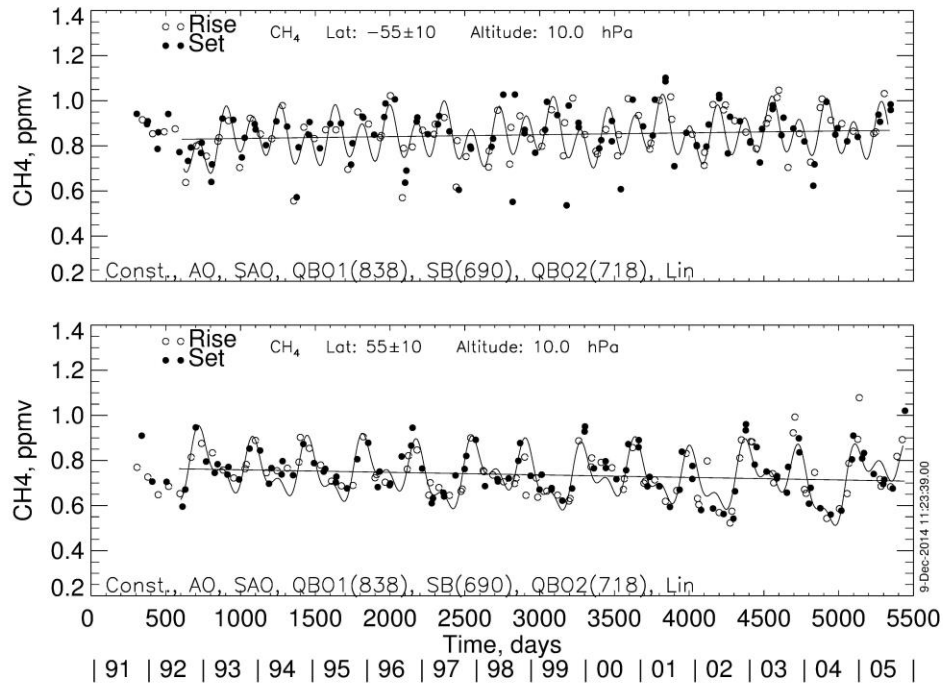
Figure 3. Time series of CH_4 is from HALOE at 10 hPa and at 55˚ latitude for the (top) southern

and for the (bottom) northern hemisphere. Solid and open circles indicate the bin-averaged CH_4

data for sunset and sunrise, respectively. The oscillating curve is the MLR fit to the data based

on the terms indicated at the lower left, and the near-horizontal line represents the sum of the

constant and linear trend terms.

7

8
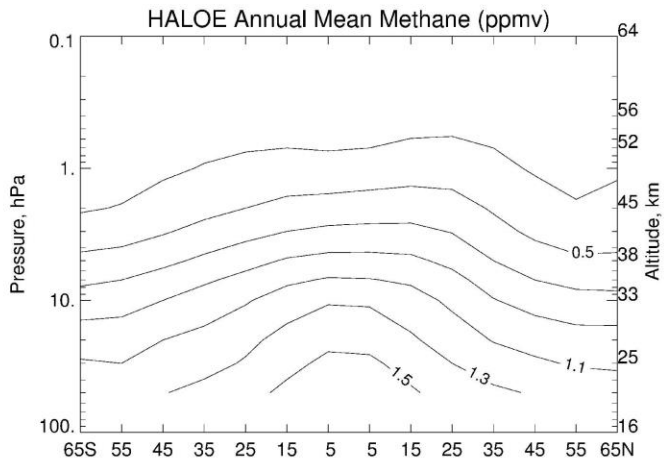
Figure 4. Annually-averaged, zonal mean HALOE methane from the MLR analyses (contour interval is 0.2 ppmv).

1
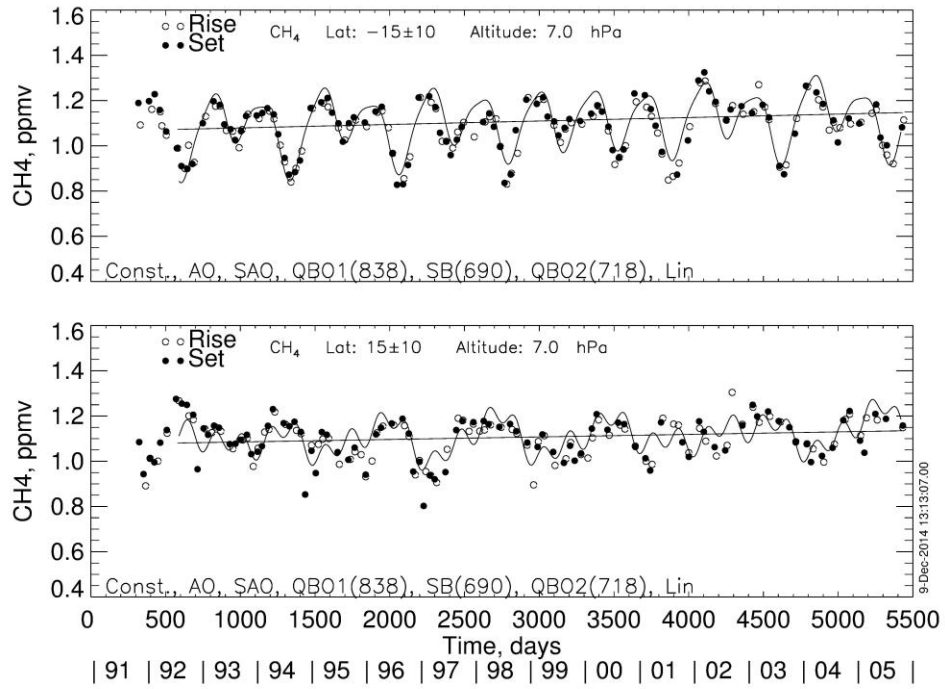
Figure 5. As in Fig. 3, but at 7 hPa and at 15˚ latitude for the (top) southern and for the (bottom)

northern hemisphere.

4

1

Linear Trends for HALOE Methane (%/decade)

2
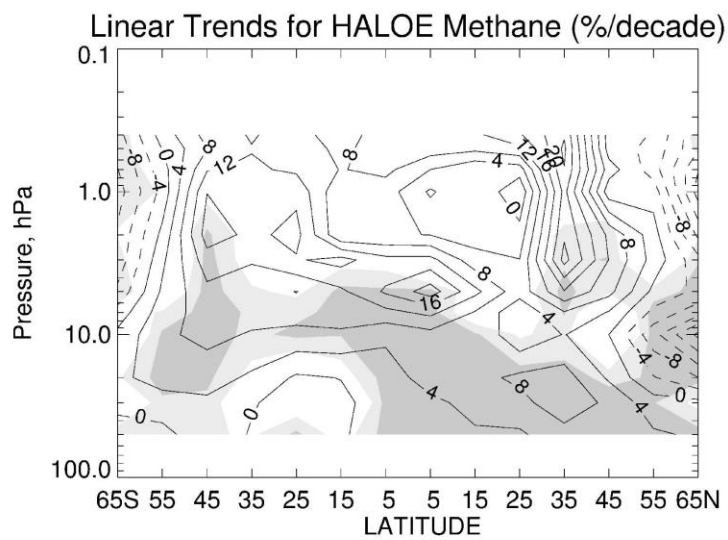
Figure 6. Linear trends for HALOE methane (in %/decade). Zero and positive trends are solid

contours and negative trends are dashed; contour interval is 4 %/decade. Dark shading denotes

where the trends have a confidence interval (CI) ≥ 90%, and lighter shading denotes 70% ≤ CI ≤

90%.

7

8
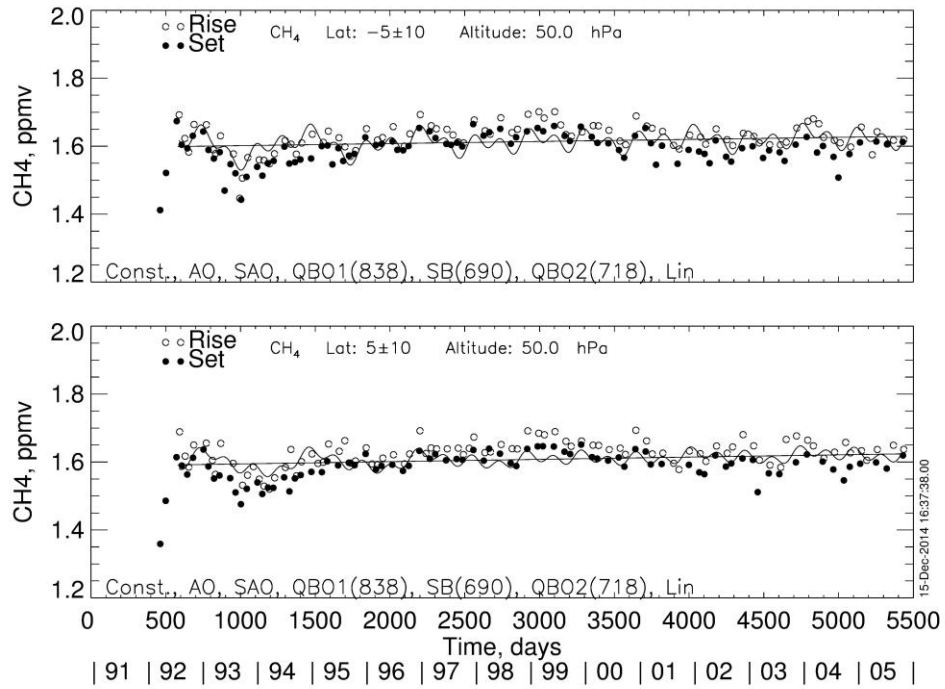
Figure 7. As in Fig. 3, but at 50 hPa and at 5˚ latitude for the (top) southern and for the (bottom) northern hemisphere.

HALOE Methane Trends, 1992-2005

1
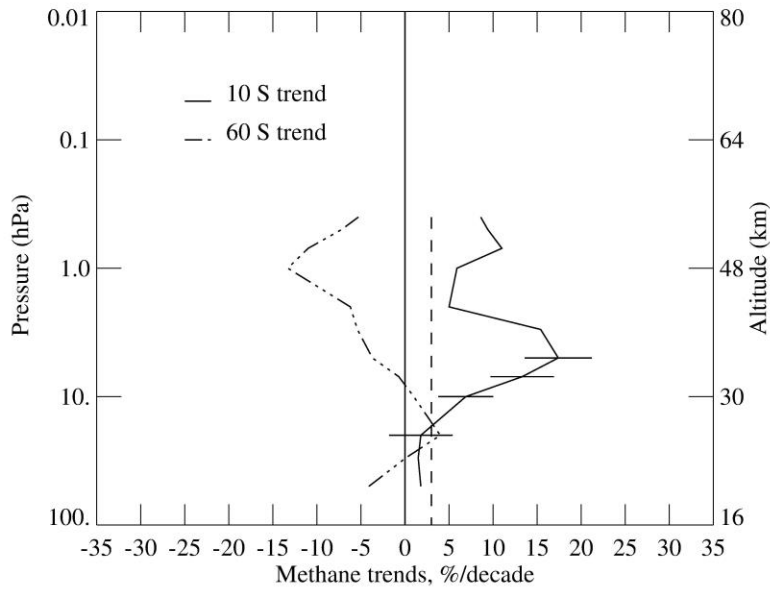
Figure 8. Tropical and high latitude trend profiles for CH_4 in the southern hemisphere. Vertical

dashed line is the approximate trend for tropospheric CH_4 or 3.0 ± 0.7 %/decade. Horizontal bars

show the 2σ error estimates for the highly significant trend terms.

5

HALOE Methane Trends, 1992-2005
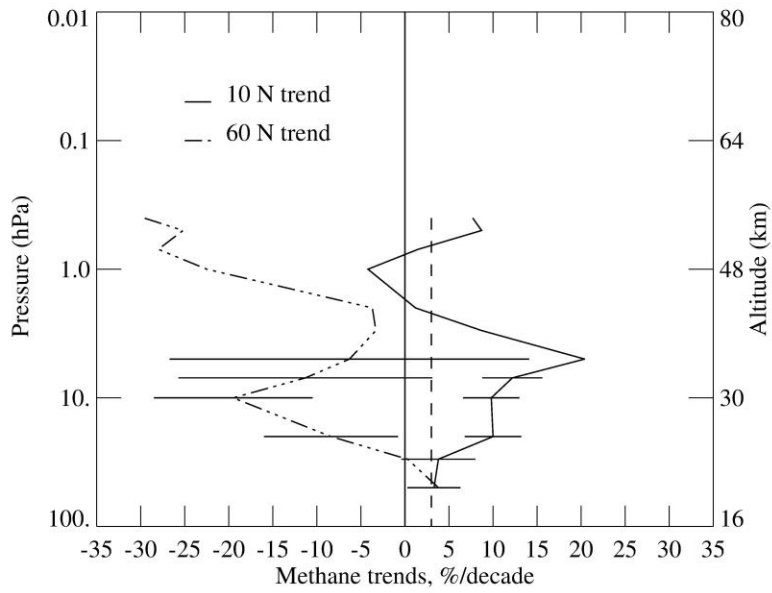
Figure 9. As in Fig. 8, but for the northern hemisphere.
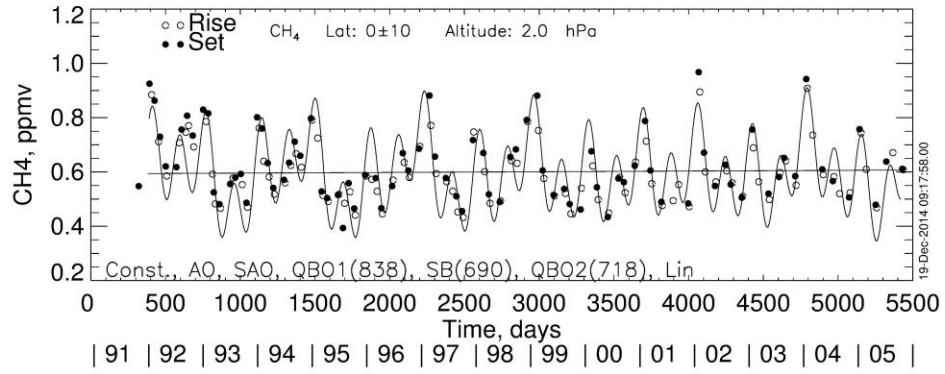
1

2 Figure 10. Time series of HALOE CH_4 at 2 hPa at the tropical latitudes for comparison with that

3 of Nedoluha et al. (1998).

4

5

Southern Extratropics (35S), 1992-2005
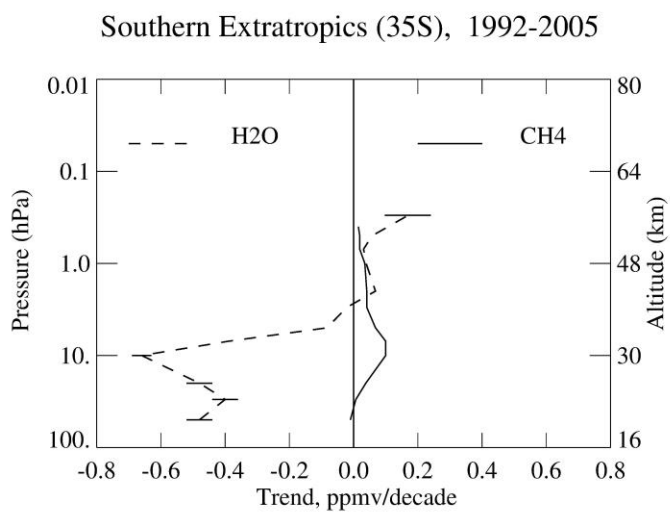
1

2   Figure 11. Trend profiles (in ppmv/decade) for CH_4 and H_2O at 35˚ latitude in the southern

3   hemisphere. Horizontal bars denote the 2σ uncertainties for the highly significant trends.

4

Northern Extratropics (35N), 1992-2005
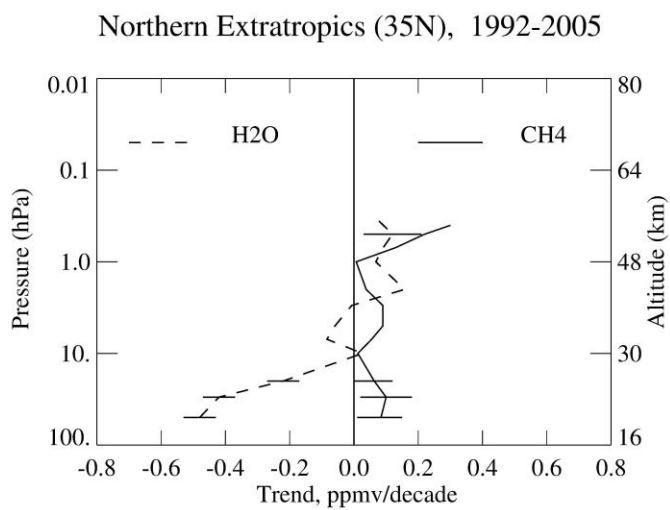
Figure 12. As in Fig. 11, but for 35˚ latitude in the northern hemisphere.

51

1


2
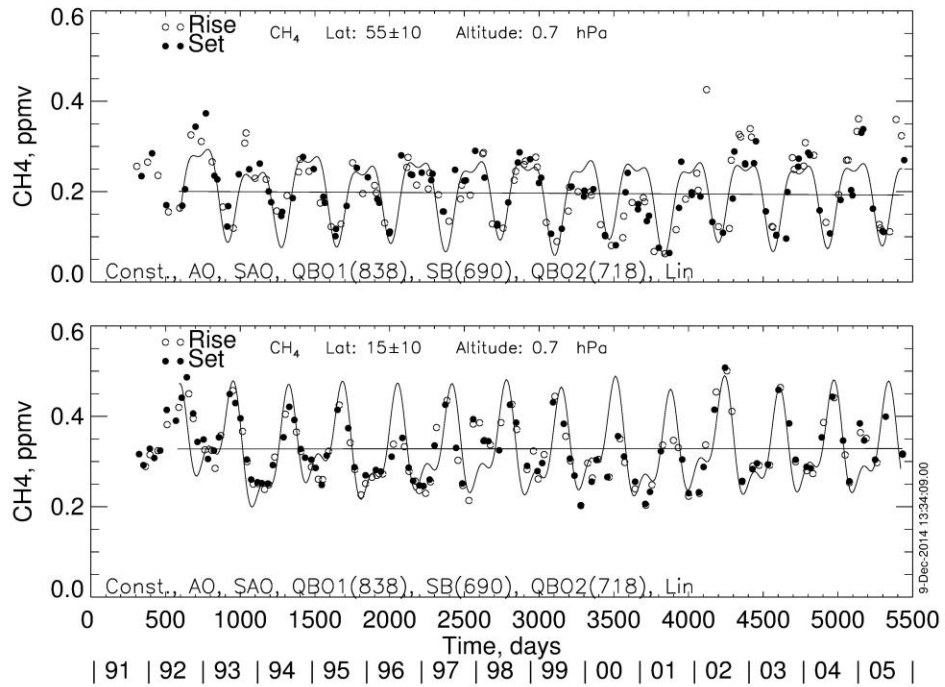
Figure 13. As in Fig. 3, but for CH$_4$ at 0.7 hPa and at the latitudes of 55˚ (top) and 15˚ (bottom)
of the northern hemisphere.

5

6

1

2

3
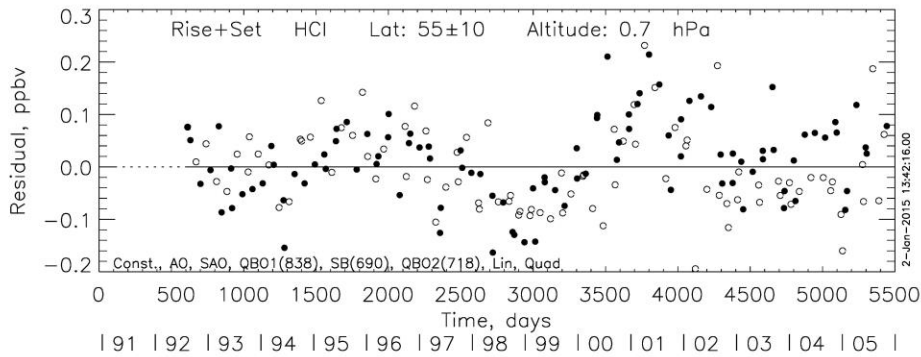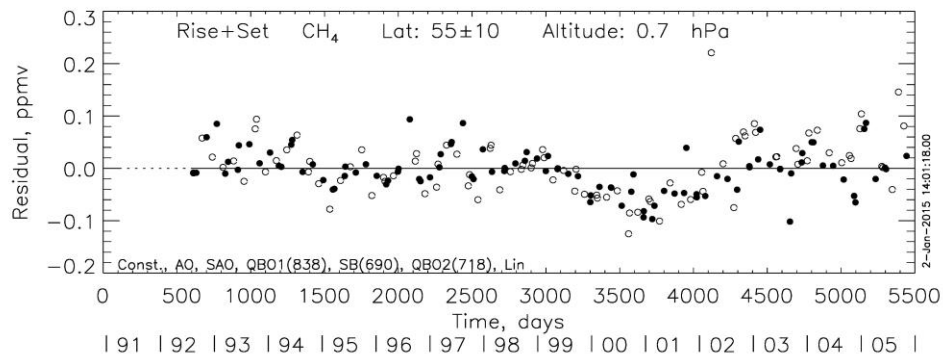
Figure 14. (top) Time series of HCl residual (data – MLR curve) at 0.7 hPa and at 55˚N;

(bottom) time series of CH_4 residual at 55˚N.

53